Article

Not peer-reviewed version

A Study on the Temperature-Dependent Behavior of Small Heat Shock Proteins from Methanogens

Nina Kurokawa , Mima Ogawa , Rio Midorikawa , Arisa Kanno , Wakaba Naka , Keiichi Noguchi , Ken Morishima , Rintaro Inoue , Masaaki Sugiyama , Masafumi Yohda *

Posted Date: 28 April 2025

doi: 10.20944/preprints202504.2381.v1

Keywords: chaperone; small heat shock protein; methanogen; analytical ultracentrifuge; stress

 doi:10.20944/preprints202504.2381.v1

Article

A Study on the Temperature-Dependent Behavior of Small Heat Shock Proteins from Methanogens

Nina Kurokawa [1], Mima Ogawa [1], Rio Midorikawa [1], Arisa Kanno [1], Wakaba Naka [1], Keiichi Noguchi [2], Ken Morishima [3], Rintaro Inoue [3], Masaaki Sugiyama [3] and Masafumi Yohda [1,*]

[1] Department of Biotechnology and Life Science, Tokyo University of Agriculture and Technology, Tokyo 184-8588, Japan

[2] Instrumentation Analysis Center, Tokyo University of Agriculture and Technology, Tokyo 184-8588, Japan

[3] Institute for Integrated Radiation and Nuclear Science, Kyoto University, Osaka 590-0494, Japan

* Correspondence: yohda@cc.tuat.ac.jp; Tel.: +81-42-388-7479

Abstract: Small heat shock proteins (sHSPs) are ubiquitous, low-molecular-weight chaperones that prevent protein aggregation under cellular stress conditions. Under normal conditions, they assemble into large oligomers. In response to stress, such as elevated temperatures, they undergo conformational changes that expose hydrophobic surfaces, allowing them to interact with denatured proteins. At heat shock temperatures in bacteria, the large sHSP oligomers disassemble into smaller oligomeric forms. Methanogens are a diverse group of microorganisms, ranging from thermophilic to psychrophilic and halophilic species. Accordingly, their sHSPs exhibit markedly different temperature dependencies based on their optimal growth temperatures. In this study, we characterized sHSPs from both hyperthermophilic and mesophilic methanogens to investigate the mechanisms underlying their temperature-dependent behavior. Using analytical ultracentrifugation, we observed the dissociation of sHSPs from a mesophilic methanogen into dimers. The dissociation equilibrium of these oligomers was found to be dependent not only on temperature but also on protein concentration. Furthermore, by generating various mutants, we identified specific amino acid residues responsible for the observed temperature dependency.

Keywords: chaperone, small heat shock protein, methanogen, analytical ultracentrifuge, stress

1. Introduction

Small heat shock proteins (sHsps) are a family of molecular chaperones with relatively low molecular weights, ranging from 12 to 43 kDa [1]. They are ubiquitously present across the biological world. Compared to other molecular chaperones, sHsps have long been underappreciated; however, recent studies have revealed their important role in maintaining intracellular proteostasis. Mutations in human sHsps have been linked to various diseases, including myopathies, neuropathies, and cataracts [2]. sHsps are characterized by the presence of an α-crystallin domain, consisting of approximately 80 amino acid residues [3]. This domain, originally identified in lens crystallin proteins, adopts a β-sandwich structure in which β-strands from adjacent subunits interact to form a stable dimer. The IXI/V motif located at the C-terminus of sHsps interacts with the α-crystallin domain of neighboring dimers, thereby promoting the formation of oligomeric structures [4].

Most small heat shock proteins (sHsps) form large oligomeric structures composed of 12 to 36 subunits [5]. However, detailed atomic-level structural information on sHsp oligomers remains limited. Archaeal sHsps typically form spherical 24-mer oligomers with a diameter of approximately 12 nm [6,7]. In contrast, the sHsp from wheat (wHsp16.9) forms a double-ring-shaped oligomer consisting of 12 subunits [8]. The sHsp from the fission yeast *Schizosaccharomyces pombe*, SpHsp16.0, assembles into a hexadecameric oligomer composed of eight dimers, forming an elongated sphere with 4-2-2 symmetry [9]. Sip1, one of the 16 sHsps identified in *Caenorhabditis elegans*, exhibits

 doi:10.20944/preprints202504.2381.v1

chaperone activity that is regulated by pH [10]. Under acidic conditions, Sip1 inhibits protein aggregation in a concentration-dependent manner. Its oligomeric structure changes in response to pH, with 24-mer, 28-mer, and 32-mer assemblies observed by cryo-electron microscopy (cryo-EM). At a low pH of 5.8, Sip1 shifts to a relatively small oligomeric form. Among these, the crystal structure of the 32-mer has been resolved. In humans, ten sHsps have been identified in the genome [11]. Recently, the crystal structure of human Hsp27 (also known as HspB1) was reported [12]. This protein forms a spherical oligomeric complex composed of 24 monomers. Each monomer features a structurally conserved α-crystallin domain consisting of a six-stranded β-sandwich, flanked by flexible N- and C-terminal regions. HspB1 from Chinese hamster exists as 18-mer or 24-mer complex and is in dynamic equilibrium with the dissociated oligomers in the hexameric unit. The hexamer further dissociates to dimers [13].

In their large oligomeric state, sHsps typically do not exhibit chaperone activity. However, under stress conditions such as elevated temperatures, they dissociate, exposing hydrophobic regions that help prevent the irreversible aggregation of denatured proteins [14]. Nevertheless, some studies suggest that complete dissociation of the oligomers is not required for the suppression of protein aggregation [15,16], and a unified mechanism for this suppression has yet to be established. In mammals, phosphorylation of serine residues in the N-terminal region allows sHsps to exhibit chaperone activity even under non-stress conditions [17]. sHsps are found in organisms across a wide range of temperature environments, from psychrophiles to hyperthermophiles. These proteins undergo structural transitions and demonstrate functional activity at temperatures exceeding the organism's optimal growth temperature. However, the precise mechanism by which sHsps sense and respond to temperature changes remains unclear. In the acidothermophilic archaeon *Sulfolobus tokodaii*, it has been reported that mutations in the IXI/V motif of its sHsp alter temperature-dependent behavior [18]. This study indicated that activation is associated with oligomer dissociation. However, since the IXI/V motif is conserved across all sHsps, this mechanism alone cannot fully account for the observed temperature dependence.

Methanogens are a group of microorganisms that produce methane under anaerobic conditions and are all classified within the domain Archaea [19]. In anaerobic environments, organic materials are decomposed through the cooperative actions of various microorganisms. Methanogenic archaea are responsible for the final step in the degradation of organic matter, generating methane from limited substrates such as hydrogen, formate, acetate, and methylamines produced by fermentative bacteria and other organisms. Methanogens are ubiquitously distributed in anaerobic habitats, including sediments of swamps and rivers, the digestive tracts of animals and insects, paddy fields, marine sediments, and anaerobic wastewater treatment reactors. They exhibit a remarkable diversity in physiological characteristics, ranging from hyperthermophilic to psychrophilic and halophilic types, making them one of the most physiologically varied groups of microorganisms. The hyperthermophilic methanogen *Methanocaldococcus jannaschii* was discovered in 1983 by the Woods Hole Oceanographic Institution at a hydrothermal vent located 2,600 meters deep in the East Pacific Ocean [20]. It is a slightly irregularly shaped, flagellated coccus that grows in seawater supplemented with sulfur at slightly acidic pH, utilizing formate or hydrogen and carbon dioxide as energy sources. Notably, it has an exceptionally fast growth rate, with a doubling time of only 25 minutes—the fastest among known methanogens. M. jannaschii grows within a temperature range of 48–86 °C, with an optimal temperature of 85 °C. Its complete genome sequence was determined in 1996 [21]. The genome of *M. jannaschii* contains a single gene encoding a small heat shock protein (sHsp). The 2.9 Å resolution crystal structure of the 24-subunit homo-oligomer MjHSP16.5 [6]. The first structure determined for an sHsp, reveals a tripartite domain architecture that represents the prevailing features seen in the sHsp family. The N-terminal domain (NTD) of MjsHSP16.5 (residues 1–43) is buried within the cavity of the protein oligomer and is notably characterized by its richness in phenylalanine residues. With the exception of residues 36–40, which form the β1 strand, the majority of residues in the NTD are disordered but predicted to adopt a helical conformation [22]. Interestingly, MjHSP16.5 retains the ability to form native-like oligomeric assemblies even when

 doi:10.20944/preprints202504.2381.v1

truncated at the N-terminal domain. A high-resolution structure of the MjHSP16.5 24-mer was also obtained using single-particle cryo-electron microscopy (cryo-EM), allowing comparison with the crystallographic structure. While both models depict a hollow spherical oligomer, the cryo-EM structure is believed to more closely represent the protein's native state. Notably, the cryo-EM model revealed density corresponding to residues Thr24–Thr33 of the NTD, a region that remains unresolved in most crystal structures [23]. At temperatures above 60 °C, the subunits of MjHSP16.5 undergo rapid and reversible exchange, with the exchange reactions showing strong temperature dependence. At 37 °C, MjHSP16.5 displays significantly lower chaperone activity compared to other sHsps. Given the high sequence similarity among methanogen-derived sHsps and their markedly different temperature-dependent behaviors, the present study was conducted to elucidate the molecular mechanism underlying the temperature responsiveness of methanogenic sHsps.

2. Results

Figure 1 shows the sequence alignment of small heat shock proteins (sHsps) from *M. jannaschii* (designated as MJsHsp in this manuscript) and *Methanococcus maripaludis*, a mesophilic methanogen (designated as MMsHsp) [24]. The genes encoding MJsHsp and MMsHsp were synthesized, and a point mutation was introduced into MJsHsp to substitute threonine at position 33 with methionine, enabling N-terminal sequence exchange. The genes were cloned into the pET23 expression vector. Using the constructed plasmids, both MJsHsp and MMsHsp were expressed in *E. coli* BL21(DE3) cells. The proteins were purified by ion exchange chromatography followed by size-exclusion chromatography. Their oligomeric states were then analyzed using high-performance liquid chromatography size-exclusion chromatography (HPLC-SEC) at room temperature and the elevated temperatures, 50°C and 60°C (Figure 1). At the room temperature, both MJsHsp and MMsHsp existed as large oligomeric complexes. At 50°C, the MJsHsp oligomer remained stable, whereas MMsHsp dissociated into smaller oligomeric forms. Since the MJsHsp oligomer was stable even up to 60°C, the T33M mutation was concluded to have minimal impact on temperature-dependent oligomer stability. We then examined the oligomeric structures of the proteins using analytical ultracentrifugation (AUC) at 40°C, the highest temperature suitable for AUC (Figure 2 and Table 1). MMsHsp existed primarily as a 24-mer, with minor proportions of 8-mer and 16-mer species. Upon dilution to 0.1 mg/ml, the proportion of the 24-mer decreased, while the amount of dimer increased. This result clearly demonstrates that, in addition to temperature, concentration also influences the dissociation equilibrium of sHsp oligomers. In contrast, MJsHsp existed predominantly as a 24-mer, along with aggregated large oligomers. There was minimal dissociation into smaller oligomers. When the concentration was reduced, the formation and dissociation of larger oligomers slightly increased.

The most significant difference between MJsHsp and MMsHsp lies in the N-terminal domain. Therefore, we created mutants with swapped N-terminal domains (Figure 1). These mutants were designated as NMCJsHsp, which is MJsHsp with the N-terminal domain of MMsHsp, and NJCMsHsp, which is MMsHsp with the N-terminal domain of MJsHsp. Contrary to our expectations, we found that the N-terminal domain is not related to the temperature dependence of oligomer stability (Figure 1).

 doi:10.20944/preprints202504.2381.v1

(a)

```
MMsHsp       MFGRDPKDPFSE-IFKVFGMGVPMEGLGGPMGKSMFQMNSMGLEISGKGFMPITLIEGDE 59
MJsHsp       MFGRDPFDSLFERMFKEF--------FATPMTGTTMIQSSMGIQISGKGFMPISIIEGDQ 52
NMCJsHsp     MFGRDPKDPFSE-IFKVFGMGVPMEGLGGPMGKSMFQMNSMGIQISGKGFMPISIIEGDQ 59
NJCMsHsp     MFGRDPFDSLFERMFKEF--------FATPMTGTTMIQSSMGLEISGKGFMPITLIEGDE 52
             ****** * : * :** *         :. **  : :  .* *::**********::*****:

MMsHsp       TIKIIALVPGINKDDIVINAIGETLELRAKRAPMAIMESEKIIYSEVPEDEEVYKTIKLP 119
MJsHsp       HIKVIAWLPGVNKEDIILNAVGDTLEIRAKRSPLMITESERIIYSEIPEEEEIYRTIKLP 112
NMCJsHsp     HIKVIAWLPGVNKEDIILNAVGDTLEIRAKRSPLMITESERIIYSEIPEEEEIYRTIKLP 119
NJCMsHsp     TIKIIALVPGINKDDIVINAIGETLELRAKRAPMAIMESEKIIYSEVPEDEEVYKTIKLP 112
              **:** :**:**:**::**:*:***:****:*: * ***:*****:**:**:*:*****

MMsHsp       APVKEGNSSAKFENGMLIVTLPKAEKAKRTGIDIE 154
MJsHsp       ATVKEENASAKFENGVLSVILPKAESSIKKGINIE 147
NMCJsHsp     ATVKEENASAKFENGVLSVILPKAESSIKKGINIE 154
NJCMsHsp     APVKEGNSSAKFENGMLIVTLPKAEKAKRTGIDIE 147
             * *** *:********:* * *****.: :.**:**
```

(b)

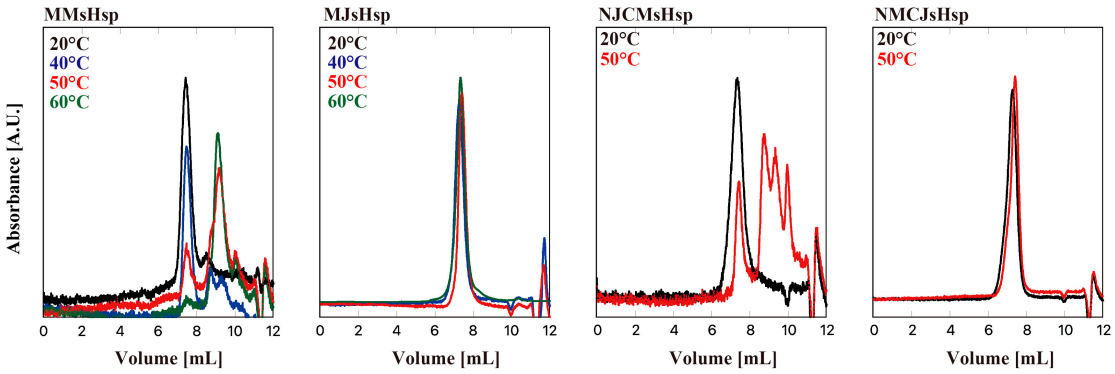

Figure 1. Sequence alignment and HPLC-SEC of MMsHsp, MJsHsp, NMCJsHsp and NJCMsHsp. (a) Sequence alignment of MMsHsp, MJsHsp, NMCJsHsp and NJCMsHsp. T33M mutation of MJsHsp is shown by blue font. The N-terminal region is enclosed in a green box. The amino acids that are mutated in this study are marked by red color. (b) Oligomeric structures of MMsHsp, MJsHsp, NMCJsHsp and NJCMsHsp were analyzed by HPLC-SEC at various temperatures. 40mM of sHsp was applied to SB-804HQ and monitored absorbance at 280 nm at 20°C and the elevated temperatures (40°C, 50°C and 60°C).

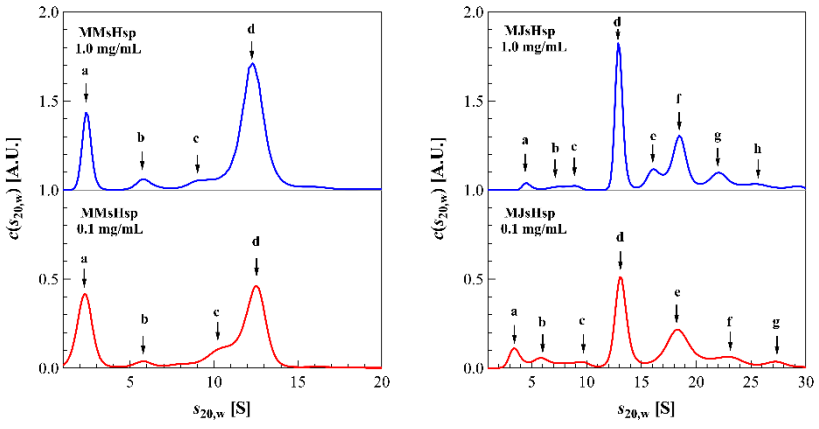

(**a**) (**b**)

Figure 2. AUC results of MJsHsp (a) and MMsHsp (b) at 40 °C. Blue and red lines represent $c(s_{20,w})$ with show the results at 1.0 mg/mL and 0.1 mg/mL, respectively.

 doi:10.20944/preprints202504.2381.v1

Table 1. Parameters obtained by AUC measurements.

MMsHsp						
c [mg/mL]	f/f_0	Peak	$s_{20,w}$ [S]	M [kDa]	N	w [%]
1.0	1.46	a	2.37	34	2	16.8
		b	5.81	132	8	4.6
		c	9.72	285	17	5.3
		d	12.33	408	24	73.3
0.1	1.43	a	2.25	31	2	31.3
		b	5.81	128	8	4.2
		c	10.31	303	18	10.9
		d	12.44	402	24	53.6
MJsHsp						
c [mg/mL]	f/f_0	Peak	$s_{20,w}$ [S]	M [kDa]	N	w [%]
1.0	1.37	a	4.57	82	5	2.1
		b	7.62	176	11	1.7
		c	8.97	225	14	2.0
		d	12.87	386	23	38.7
		e	16.08	540	33	8.8
		f	18.45	663	40	27.6
		g	22.01	864	52	12.1
		h	25.39	1071	65	7.0
0.1	1.36	a	3.39	52	3	7.3
		b	5.76	114	7	5.7
		c	9.48	242	15	4.8
		d	13.04	391	24	35.7
		e	18.28	648	39	30.7
		f	23.02	916	55	10.6
		g	27.26	1179	71	5.2

* c: concentration, f/f_0: friction ratio, $s_{20,w}$: reduced sedimentation coefficient in pure water at 20°C, M: molecular mass, N: association number, w: weight fraction.

Next, we investigated the citrate synthase (CS) aggregation suppression activity of MMsHsp and NJCMsHsp. We did not examine the chaperone activity of MJsHsp, as it is expected to show chaperone activity at the heat stress temperature for *M. jannaschii*. Curiously, MMsHsp exhibited almost no CS aggregation suppression activity (Figure 3), while NJCMsHsp showed significant aggregation suppression activity. However, MMsHsp did demonstrate insulin aggregation suppression activity. This result suggests that the N-terminal domain plays a role in the interaction with denatured proteins.

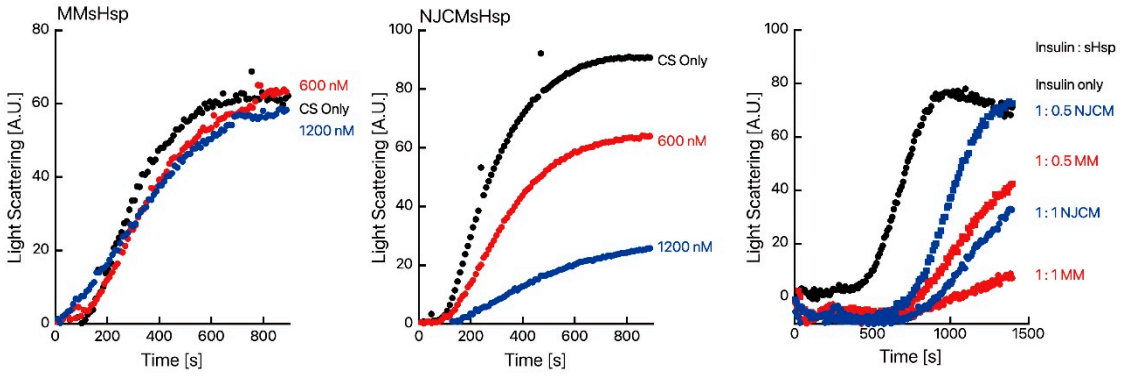

(**a**) (**b**) (c)

Figure 3. Chaperone function of MMsHsp and NJCMsHsp. The thermal aggregation of CS from the porcine heart was monitored by measuring light scattering at 500 nm with a spectrofluorometer at 50 °C. CS (50 mM, monomer) was incubated in assay buffer with or without MMsHsp (a) or NJCMsHsp (b) at the specified

 doi:10.20944/preprints202504.2381.v1

concentration. (c) 50 μM of insulin was treated with DDT with or without MMsHsp or NJCMsHsp at the specified concentration. Aggregation of Insulin was monitored by measuring light scattering at 360 nm with a spectrofluorometer at 30°C

By comparing the sequences of MJsHsp with three sHsps from mesophilic methanogens, including MMsHsp, we identified four amino acid residues that may be responsible for the temperature dependency. These residues are Q36, Q52, E118, and N145 in MJsHsp, which correspond to E43, E59, G118, and D152 in MMsHsp, respectively (Figure 1). We then created mutants of MJsHsp and MMsHsp with these amino acid substitutions: MJsHsp-Q36E, MJsHsp-Q52E, MJsHsp-E118G, MJsHsp-N145D, MMsHsp-E43Q, MMsHsp-E59Q, MMsHsp-G125E, and MMsHsp-D152N. Their temperature dependencies are shown in Figure 4. Among the four MMsHsp mutants, MMsHsp-E43Q, MMsHsp-G125E, and MMsHsp-D152N showed a slight increase in oligomer stability compared to the wild type at 50°C, while MMsHsp-E59Q had almost no effect. In contrast, we did not observe oligomer dissociation in the MJsHsp mutants at 50°C. Interestingly, the oligomer peaks were broadened, indicating partial aggregation, which may correspond to the aggregated complexes observed in AUC.

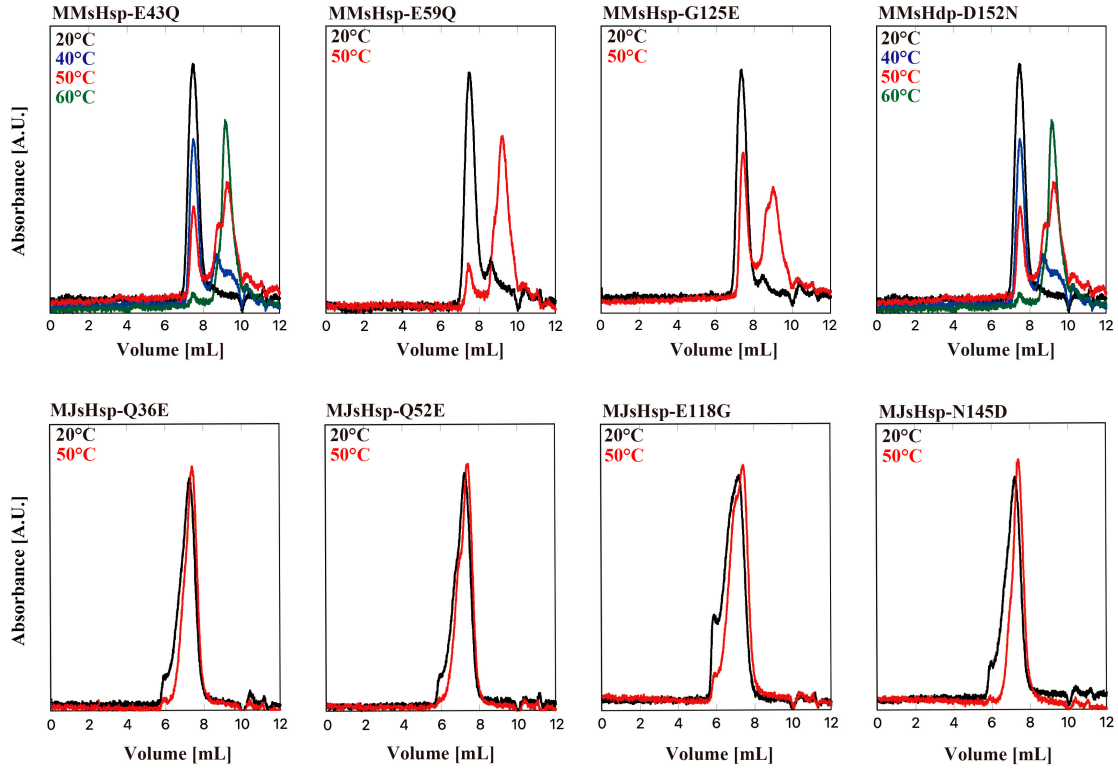

Figure 4. HPLC-SEC of single mutants of MMsHsp and MIsHsp. Oligomeric structures of single mutants of MMsHsp and MJsHsp were analyzed by HPLC-SEC at various temperatures. 40nmol of sHsp variant was applied to SB-804HQ and monitored absorbance at 280 nm at 20°C and the elevated temperatures (40, 50 and 60°C).Aggregation of Insulin was monitored by measuring light scattering at 360 nm with a spectrofluorometer at 30°C

We then examined the effects of double and triple mutations (Figure 5). The double mutation, E43Q & D152N, significantly improved the stability of MMsHsp. In contrast, the oligomer stability of MJsHsp at 50°C was not affected by the corresponding double mutation (Q36E & N145D). We also applied double mutations to the N-terminal swap mutants. The oligomer of NMCJsHsp-Q36E & N145D remained stable at 50°C. Interestingly, the peak area of NJCMsHsp-E43Q & D152N decreased at both 50°C and 60°C. This is likely due to nonspecific interactions with the HPLC column. Significant oligomer stabilization was observed in MMsHsp_E43Q & G125E & D152N (MMsHsp-3M). Partial dissociation of the MJsHsp-Q36E & E118G & N145D (MJsHsp-3M) oligomer was

 doi:10.20944/preprints202504.2381.v1

observed at 50°C, with dissociation becoming more pronounced at 60°C. Since we observed aggregation in the MJ mutants, likely due to the exposure of hydrophobic surfaces, we used a buffer containing 20% ethylene glycol for HPLC-SEC of MJsHsp-3M. The NMCJ-Q36E&E118G&N145D (MMCJ-3M) oligomer was stable at 50°C but partially dissociated at 60°C.

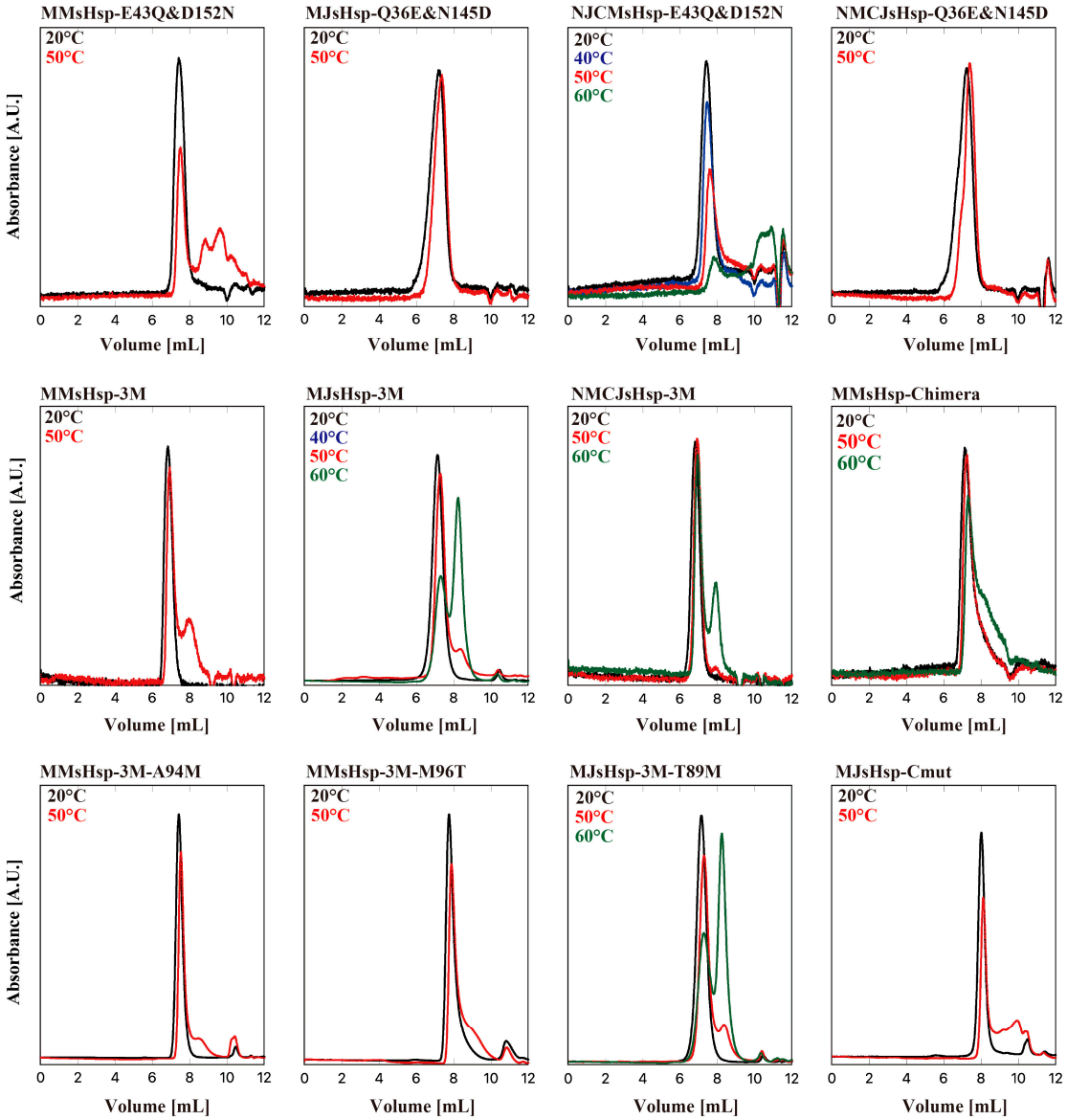

Figure 5. HPLC-SEC of double, triple, quad mutants, MMsHsp-Chimera and MJsHsp-Cmut.

Although the temperature dependency changed significantly, the oligomers of MJsHsp-3M and NMCJ-3M remained stable compared to MMsHsp at 50°C. Therefore, we attempted to identify the region responsible for the temperature dependency by constructing chimera mutants of NMCJsHsp-3M and MMsHsp-3M. The chimera mutants were constructed using the In-fusion method, incorporating the conserved five amino acids in the α-crystallin domain [24]. As shown in Supplementary Figure S1, the chimera mutant (MMsHsp-Chimera) is identical to MMsHsp-3M except for the amino acid residues between Ile-42 and Arg100, which correspond to Ile-35 and Arg-93 in MJsHsp. The oligomer of MMsHsp-Chimera exhibited higher stability at 50°C compared with MMsHsp-3M, suggesting that the amino acids between Ile-35 and Arg-93 in MJsHsp also contribute to oligomer stability (Figure 5). The amino acid sequence in this region is highly homologous. We focused on Met-87 and Thr-89 in MJsHsp, and the corresponding residues in MMsHsp-3M were mutated to those of MJsHsp. The mutants, MMsHsp-3M&A94M and MMsHsp-3M&M96T, exhibited

 doi:10.20944/preprints202504.2381.v1

a slight increase in oligomer stability at 50°C compared with MMsHsp-3M (Figure 5). Contrary to the expectations, the MJsHsp-3M&T89M mutant showed almost the same stability as MJsHsp-3M (Figure 5).

To investigate the effect of other amino acid residues, we compared the sequences of sHsps from various methanogens (Supplementary Figure S2). We found that the amino acid residues adjacent to the IXI/V motif appear to be related to temperature dependency. To clarify the effect of amino acid substitutions near the IXI motif, we performed computational docking simulations between the monomer protein and the C-terminal peptide (residues 141–147) and calculated the binding free energy (ΔG) (Table 2). The analysis revealed a decrease in the absolute ΔG value due to amino acid substitutions. The RRGINIE sequence from thermophilic methanogens showed a lower absolute ΔG compared to the KKGINIE sequence from hyperthermophilic methanogens, while the RTGIDIE sequence from mesophilic methanogens exhibited the lowest absolute ΔG. Notably, the 141-Lys and 142-Lys substitution emerged as a key determinant of this trend, suggesting that it plays a critical role in regulating binding affinity. We then constructed a mutant of MJsHsp, replacing the amino acid residues adjacent to the IXI motif, designated MJsHsp-Cmut (MJsHsp-K141R&K142T&N145D). The MJsHsp-Cmut oligomer partially dissociated at 50°C (Figure 5).

Table 2. Interaction energy between C-terminus and α-crystallin calculated by AutoDock vina.

sHsp	Mutation	Sequence	ΔG (Kcal/mol)	ΔΔG
Hyperythermophilic	WT	KKGINIE	-12.87	-
Mutant 1	N145D	KKGIDIE	-12.81	0.059
Mutant 2	K142T	KTGINIE	-12.65	0.223
Mutant 3	K141R	RKGINIE	-12.53	0.346
Thermophilc	K141R/K142R	RRGINIE	-12.68	0.189
Mesophilic	K141R/K142T/N145D	RTGIDIE	-12.41	0.458

Finally, we decided to combine various mutations. For this purpose, we used NMCJsHsp due to the issues caused by the hydrophobic nature of the N-terminus of MJsHsp. The constructed mutant, NMCJsHsp-Mut, contains amino acid mutations of Q36E, S84A, L86M, M87A, T89M, E118G, S138K, S139A, I140K, K141R, K142T and N145D (The numbers correspond to those of MJsHsp) in addition to N-terminus replacement. NMCJsHsp-Mu exhibited significant oligomer dissociation at 50°C compared to MJsHsp-3M&T89M. At 60°C, its oligomer completely dissociated into small oligomers (Figure 6).

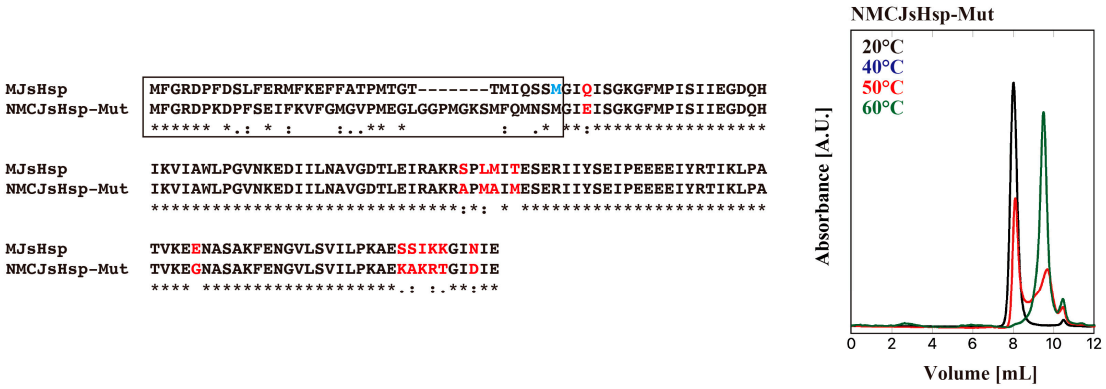

Figure 6. Sequence alignment and HPLC-SEC of NMCJsHsp-Mut.

3. Discussion

The X-ray crystal structure of MjHSP16.5 (MJsHsp) has been determined, excluding the N-terminal domain. The dimer serves as the structural unit, with the IXI motif in the C-terminal domain inserted into the groove between two β-strands of an adjacent dimer. Although the structure of MmHsp (MMsHsp) has not yet been experimentally resolved, AUC analysis indicates that MMsHsp

 doi:10.20944/preprints202504.2381.v1

also forms a 24-mer oligomer, similar to MJsHsp. Furthermore, the monomer structure predicted by AlphaFold3 closely resembles that of MJsHsp. These findings suggest that MMsHsp likely adopts a structure nearly identical to that of MJsHsp.

Unexpectedly, the N-terminal region—where the sequences of MJsHsp and MMsHsp differ the most—had little to no effect on oligomer stability. Since the N-terminal region adopts a largely disordered conformation within the oligomer, it is not directly involved in oligomer formation. A previous study has shown that an N-terminal deletion mutant adopts a structure nearly identical to that of the wild type [25] .

In the crystal structure of MjHsp16.5 (MJsHsp), Q36 is positioned in close proximity between adjacent dimers (Supplementary Figure S3). We hypothesize that substituting this residue with glutamic acid introduces electrostatic repulsion, thereby destabilizing the oligomer. N145 and E118 in MJsHsp is located at the interaction site of the C-terminal IXI motif, a region known to be critical for oligomer assembly (Supplementary Figure S4). We propose that mutations at this site may disrupt the interaction between the IXI motif and the adjacent dimer. S138, S139 I140 , K141 and K142 are also located close to the C-terminus and seem to be interaction with adjacent dimer (Supplementary Figure S5).

In the crystal structure of MJsHsp, S84, L86, M87 and T89 are located in a loop region within the α-crystallin domain. This loop lies within the dimer interface and is believed to interact with the β-strand of the adjacent monomer (Supplementary Figure S6). This loop region should be important for maintaining the stability of the oligomeric structure.

It has been shown that MJsHsp undergoes subunit exchange. Although the efficiency of subunit exchange at 40°C is expected to be low, it is believed that the exchange occurs at a certain rate. In this case, the N-terminal region is temporarily exposed, which could lead to the formation of aggregates. In contrast, MMsHsp does not form such aggregates due to its lower hydrophobicity at the N-terminal. It is likely that MJsHsp has adapted to high temperatures, and in a high-temperature environment with intense molecular motion, hydrophobic interactions with denatured proteins are strengthened. Additionally, the formation of large oligomers by MJsHsp is thought to result from the exposure of hydrophobic sites when partially dissociated, leading to the formation of large oligomers.

4. Materials and Methods

Creation of genes for wild type and mutant sHsps

The genes for MJsHsp, MMsHsp, MJsHsp-Cmut, and NMCJsHsp-mut were synthesized. They are codon optimized for the expression in *E.coli*. The nucleotide and amino acid sequences of MJsHsp and MMsHsp are shown in Supplementary Figure S7. To facilitate the construction of the N-terminal domain exchange variant, NcoI site were introduced resulting in the replacement of Thr-33 to Met in MJsHsp. Point mutations were introduced by the DpnI mediated site-directed Mutagenesis [26]. The In-Fusion method was used to generate the chimeras [27]. The used primers are shown in Supplementary Table. The genes of wild-type and mutant sHsp were cloned into a pET23 vector and expressed in *E. coil* BL21(DE3). The expressed sHsps were purified by anion exchange chromatography using DEAE-650 and TOYOPEARL SuperQ-650 and gel filtration chromatography using Superdex 200. Glycerol was added to the samples to a final concentration of 20 %, frozen in liquid nitrogen, and stored at -30 or -80°C.

HPLC-SEC

HPLC-SEC was performed with a gel filtration column (SB-804HQ, Showa Denko, Tokyo, Japan) using an HPLC system, PU-1580i, connected to an MD1515 multiwavelength detector or UV/Vis detector UV4075 as described previously [18]. The sHsp variants were heated at the specified temperature for 30 min and then loaded onto a column heated at the same temperature and eluted with buffer B with or without 20% ethylene glycol at a flow rate of 0.5 mL/min. The proteins are monitored by the absorbance at 220 nm or 280 nm.

AUC measurements

 doi:10.20944/preprints202504.2381.v1

AUC measurements were carried out with ProteomeLab XL-I (Beckman Coulter, Brea, CA, USA). Samples were filled in 12 mm pathlength aluminum double sector centerpieces. All measurements were performed in the sedimentation velocity mode using Rayleigh interference optics at a 40,000 rpm rotor speed. The time evolution of sedimentation data was analyzed with the multi components Lamm formula. Then the weight concentration distribution of components, $c(s_{20,w})$, was obtained as a function of the sedimentation coefficient. Here, the sedimentation coefficient was normalized to be the value at 20 °C in pure water, $s_{20,w}$. The molecular mass M and association number N of each component were calculated using the following equation.

$$\boldsymbol{M = \left[\frac{6\pi\eta N_A}{(1-\rho\bar{v})}\right]^{1.5}\left(\frac{3\bar{v}}{4\pi N_A}\right)^{0.5}\left(\frac{f}{f_0}\right)^{1.5} s_{20,w}{}^{1.5}}, (1)$$

$$\boldsymbol{N = \frac{M}{M_1}}, (2)$$

where ρ, η, $\bar{v}$, N_A, f/f_0, and M_1,,are the solvent density of pure water at 20 °C, solvent viscosity of pure water at 20 °C, partial specific volume, Avogadro number, friction ratio, molecular mass of a monomer, respectively. These calculations were performed with SEDFIT software [28]. The density and viscosity of solvents were measured with a density meter DMA4500M (Anton Paar, Graz, Austria) and a viscometer Lovis 2000 M/ME (Anton Paar, Graz, Austria), respectively.

Protein aggregation measurements

The thermal aggregation of citrate synthase from the porcine heart (CS) was monitored by measuring light scattering at 500 nm with a spectrofluorometer (FP-6500, JASCO, Tokyo, Japan) at 50 °C as described previously [13]. Native CS (50 nM, monomer) was incubated in TKM buffer (50 mM Tris-HCl, pH 7.5, 100 mM KCl, and 25 mM MgCl2) with or without sHsp. The assay buffer was preincubated at 50 °C and continuously stirred throughout the measurement.

The activity of inhibiting insulin aggregation was evaluated by measuring the time-dependent change in absorbance at 360 nm using a spectrofluorometer (FP-6500) equipped with a thermostatted cell. First, insulin was dissolved in a buffer (25 mM HCl, 100 mM NaCl) to a concentration of 2 mg/mL. Then, 2× buffer (Sodium phosphate (pH 6.8), 300 mM NaCl, 0.5 mM EDTA) was added to a four-sided quartz cell, and the sample was added in a mass ratio (Insulin : sHsp = 1:0.5, 1:1). The sample was pre-incubated for 10 minutes at 30°C. Afterward, DTT was added to achieve a final concentration of 20 mM, and insulin was added to reach a final concentration of 50 μM. Absorbance at 360 nm was measured for 1400 seconds. During the measurement, the cell was stirred at 250 rpm, and the reaction temperature was maintained at 30°C.

Monomer–C-terminal Domain Docking Simulation

The three-dimensional structural data of MJsHsp was obtained from the RCSB Protein Data Bank (www.rcsb.org) with the PDB code entry 4I88. Monomer and C-terminal residues from positions 141 to 147 were extracted using PyMOL2. Subsequently, amino acid residues within the C-terminal peptide were substituted as needed. The three-dimensional structural data of the extracted monomer and C-terminal peptide were prepared using AutoDockTools by adding hydrogen atoms and computing Gasteiger charges. Docking of the MJsHSP monomer with the C-terminal peptide (residues 141-147) was performed using the empirical free energy function and the Iterated Local Search global optimization algorithm implemented in AutoDock vina [29]. The grid box for the docking process was set up using AutoDockTools, with grid dimensions of 40Å × 40Å × 40Å, centered between the beta sheets around positions 70 and 120 of the monomer. A spacing of 0.375 Å was used. The docking parameters included an exhaustiveness value of 8, with 100 binding modes (num_modes) generated and an energy range of 3 kcal/mol. The binding pose and binding free energy ΔG (kcal/mol) of the lowest energy binding mode were calculated.

Supplementary Materials: The following supporting information can be downloaded at the website of this paper posted on Preprints.org, Supplementary Figure S1, S2, S3, S4, S5, S6 , S7 and Supplementary Table.

 doi:10.20944/preprints202504.2381.v1

Author Contributions: Conceptualization, M.Y.; data curation, M.S. and M.Y.; funding acquisition, M.Y., K.M., R.I., and M.S; investigation, N.K., M.O., R.M., A.K., W.N., K.N., K.M., R.I., and M.S.; methodology, M.S. and M.Y.; project administration, M.Y.; supervision, M.Y.; validation, M.Y.; writing—original draft preparation, M.Y.; writing—review and editing, M.Y. All authors have read and agreed to the published version of the manuscript.

Funding: This work was partially supported by JSPS KAKENHI, grant numbers 18H04690, and 20H02532 to M.Y., 21K15051 and 25K09577 to K.M., 19KK0071 and 20K06579 to R.I., 18H05229 and 18H03681 to M.S. and Platform Project for Supporting Drug Discovery and Life Science Research [Basis for Supporting Innovative Drug Discovery and Life Science Research (BINDS)] from AMED (award No. JP22ama121001j0001 to M.S.).

Acknowledgments: AUC experiment at Institute for Integrated Radiation and Nuclear Science, Kyoto University (KURNS) were per-formed under proposal numbers 31083, R3005, R4083, R5041, R6029.

Conflicts of Interest: The authors declare no conflicts of interest.

Abbreviations

MJsHsp sHsp of *Methanocaldococcus jannaschii* with T33M mutation

MMsHsp sHsp of *Methanococcus maripaludis*

HPLC-SEC High-performance liquid chromatography size-exclusion chromatography (HPLC-SEC)

AUC Analytical ultracentrifugation (AUC)

CS Citrate synthase from porcine heart

NMCJsHsp MJsHsp with the N-terminal domain of MMsHsp

NJCMsHsp MMsHsp with the N-terminal domain of MJsHsp

MJsHsp-Q36E MJsHsp with Q36E mutation

MJsHsp-Q52E MJsHsp with Q52E mutation

MJsHsp-E118G MJsHsp with E118G mutation

MJsHsp-N145D MJsHsp with N145D mutation

MMsHsp-E43Q MMsHsp with E43Q mutation

MMsHsp-E59Q MMsHsp with E59Q mutation

MMsHsp-G125E MMsHsp with G125E mutation

MMsHsp-D152N MMsHsp with D152N mutation

MMsHsp MMsHsp with E43Q and D152N mutations

MJsHsp MJsHsp with Q36E and N145D mutations

NJCMsHsp NJCMsHsp with E43Q and D152N mutations

NMCJsHsp NMCJsHsp with Q36E and N145D mutations

MMsHsp-3M MMsHsp with E43Q, G125E and D152 mutations

MJsHsp-3M MJsHsp with Q36E, E118G and N145D mutations

NMCJsHsp-3M NMCJsHsp with Q36E, E118G and N145D mutations

MMsHsp-Chimera A chimera sHsp of NMCJsHsp-3M and MMsHsp-3M

MMsHsp-3M-A94M MMsHsp with E43Q, A94M, G125E and D152 mutations

MMsHsp-3M-M96T MMsHsp with E43Q, M96T, G125E and D152 mutations

MJsHsp-3M-T89M MJsHsp with Q36E, T89M and N145D mutations

MJsHsp-Cmut MJsHsp with K141R, K142T and N145D mutations

NMCJsHsp-Mut NMCJsHsp with Q36E, S84A, L86M, M87A, T89M, E118G, S138K, S139A, I140K, K141R, K142T and N145D mutations

 doi:10.20944/preprints202504.2381.v1

References

1. Garrido, C.; Paul, C.; Seigneuric, R.; Kampinga, H. H., The small heat shock proteins family: the long forgotten chaperones. *Int J Biochem Cell Biol* **2012,** 44, (10), 1588-92.
2. Bakthisaran, R.; Tangirala, R.; Rao Ch, M., Small heat shock proteins: Role in cellular functions and pathology. *Biochim Biophys Acta* **2015,** 1854, (4), 291-319.
3. Caspers, G. J.; Leunissen, J. A.; de Jong, W. W., The expanding small heat-shock protein family, and structure predictions of the conserved "alpha-crystallin domain". *J Mol Evol* **1995,** 40, (3), 238-48.
4. Delbecq, S. P.; Jehle, S.; Klevit, R., Binding determinants of the small heat shock protein, alphaB-crystallin: recognition of the 'IxI' motif. *EMBO J* **2012,** 31, (24), 4587-94.
5. Santhanagopalan, I.; Degiacomi, M. T.; Shepherd, D. A.; Hochberg, G. K. A.; Benesch, J. L. P.; Vierling, E., It takes a dimer to tango: Oligomeric small heat shock proteins dissociate to capture substrate. *J Biol Chem* **2018,** 293, (51), 19511-19521.
6. Kim, K. K.; Kim, R.; Kim, S. H., Crystal structure of a small heat-shock protein. *Nature* **1998,** 394, (6693), 595-9.
7. Hanazono, Y.; Takeda, K.; Yohda, M.; Miki, K., Structural studies on the oligomeric transition of a small heat shock protein, StHsp14.0. *J Mol Biol* **2012,** 422, (1), 100-8.
8. van Montfort, R. L.; Basha, E.; Friedrich, K. L.; Slingsby, C.; Vierling, E., Crystal structure and assembly of a eukaryotic small heat shock protein. *Nat Struct Biol* **2001,** 8, (12), 1025-30.
9. Hanazono, Y.; Takeda, K.; Oka, T.; Abe, T.; Tomonari, T.; Akiyama, N.; Aikawa, Y.; Yohda, M.; Miki, K., Nonequivalence observed for the 16-meric structure of a small heat shock protein, SpHsp16.0, from Schizosaccharomyces pombe. *Structure* **2013,** 21, (2), 220-8.
10. Fleckenstein, T.; Kastenmuller, A.; Stein, M. L.; Peters, C.; Daake, M.; Krause, M.; Weinfurtner, D.; Haslbeck, M.; Weinkauf, S.; Groll, M.; Buchner, J., The Chaperone Activity of the Developmental Small Heat Shock Protein Sip1 Is Regulated by pH-Dependent Conformational Changes. *Mol Cell* **2015,** 58, (6), 1067-78.
11. Kappe, G.; Franck, E.; Verschuure, P.; Boelens, W. C.; Leunissen, J. A.; de Jong, W. W., The human genome encodes 10 alpha-crystallin-related small heat shock proteins: HspB1-10. *Cell Stress Chaperones* **2003,** 8, (1), 53-61.
12. Nappi, L.; Aguda, A. H.; Nakouzi, N. A.; Lelj-Garolla, B.; Beraldi, E.; Lallous, N.; Thi, M.; Moore, S.; Fazli, L.; Battsogt, D.; Stief, S.; Ban, F.; Nguyen, N. T.; Saxena, N.; Dueva, E.; Zhang, F.; Yamazaki, T.; Zoubeidi, A.; Cherkasov, A.; Brayer, G. D.; Gleave, M., Ivermectin inhibits HSP27 and potentiates efficacy of oncogene targeting in tumor models. *J Clin Invest* **2020,** 130, (2), 699-714.
13. Kurokawa, N.; Midorikawa, R.; Nakamura, M.; Noguchi, K.; Morishima, K.; Inoue, R.; Sugiyama, M.; Yohda, M., Oligomeric Structural Transition of HspB1 from Chinese Hamster. *Int J Mol Sci* **2021,** 22, (19).
14. Hirose, M.; Tohda, H.; Giga-Hama, Y.; Tsushima, R.; Zako, T.; Iizuka, R.; Pack, C.; Kinjo, M.; Ishii, N.; Yohda, M., Interaction of a small heat shock protein of the fission yeast, Schizosaccharomyces pombe, with a denatured protein at elevated temperature. *J Biol Chem* **2005,** 280, (38), 32586-93.
15. Franzmann, T. M.; Wuhr, M.; Richter, K.; Walter, S.; Buchner, J., The activation mechanism of Hsp26 does not require dissociation of the oligomer. *J Mol Biol* **2005,** 350, (5), 1083-93.
16. Abe, T.; Oka, T.; Nakagome, A.; Tsukada, Y.; Yasunaga, T.; Yohda, M., StHsp14.0, a small heat shock protein of Sulfolobus tokodaii strain 7, protects denatured proteins from aggregation in the partially dissociated conformation. *J Biochem* **2011,** 150, (4), 403-9.
17. Kostenko, S.; Moens, U., Heat shock protein 27 phosphorylation: kinases, phosphatases, functions and pathology. *Cell Mol Life Sci* **2009,** 66, (20), 3289-307.

 doi:10.20944/preprints202504.2381.v1

18. Saji, H.; Iizuka, R.; Yoshida, T.; Abe, T.; Kidokoro, S.; Ishii, N.; Yohda, M., Role of the IXI/V motif in oligomer assembly and function of StHsp14.0, a small heat shock protein from the acidothermophilic archaeon, Sulfolobus tokodaii strain 7. *Proteins* **2008,** 71, (2), 771-82.
19. Liu, Y.; Whitman, W. B., Metabolic, phylogenetic, and ecological diversity of the methanogenic archaea. *Ann N Y Acad Sci* **2008,** 1125, 171-89.
20. Jones, W. J.; Leigh, J. A.; Mayer, F.; Woese, C. R.; Wolfe, R. S., Methanococcus-Jannaschii Sp-Nov, an Extremely Thermophilic Methanogen from a Submarine Hydrothermal Vent. *Archives of Microbiology* **1983,** 136, (4), 254-261.
21. Bult, C. J.; White, O.; Olsen, G. J.; Zhou, L.; Fleischmann, R. D.; Sutton, G. G.; Blake, J. A.; FitzGerald, L. M.; Clayton, R. A.; Gocayne, J. D.; Kerlavage, A. R.; Dougherty, B. A.; Tomb, J. F.; Adams, M. D.; Reich, C. I.; Overbeek, R.; Kirkness, E. F.; Weinstock, K. G.; Merrick, J. M.; Glodek, A.; Scott, J. L.; Geoghagen, N. S.; Venter, J. C., Complete genome sequence of the methanogenic archaeon, Methanococcus jannaschii. *Science* **1996,** 273, (5278), 1058-73.
22. Shi, J.; Koteiche, H. A.; McDonald, E. T.; Fox, T. L.; Stewart, P. L.; McHaourab, H. S., Cryoelectron microscopy analysis of small heat shock protein 16.5 (Hsp16.5) complexes with T4 lysozyme reveals the structural basis of multimode binding. *J Biol Chem* **2013,** 288, (7), 4819-30.
23. Lee, J.; Ryu, B.; Kim, T.; Kim, K. K., Cryo-EM structure of a 16.5-kDa small heat-shock protein from Methanocaldococcus jannaschii. *Int J Biol Macromol* **2024,** 258, (Pt 1), 128763.
24. Jones, W. J.; Whitman, W. B.; Fields, R. D.; Wolfe, R. S., Growth and plating efficiency of methanococci on agar media. *Appl Environ Microbiol* **1983,** 46, (1), 220-6.
25. Usui, K.; Hatipoglu, O. F.; Ishii, N.; Yohda, M., Role of the N-terminal region of the crenarchaeal sHsp, StHsp14.0, in thermal-induced disassembly of the complex and molecular chaperone activity. *Biochem Biophys Res Commun* **2004,** 315, (1), 113-8.
26. Fisher, C. L.; Pei, G. K., Modification of a PCR-based site-directed mutagenesis method. *Biotechniques* **1997,** 23, (4), 570-1, 574.
27. Zhu, B.; Cai, G.; Hall, E. O.; Freeman, G. J., In-fusion assembly: seamless engineering of multidomain fusion proteins, modular vectors, and mutations. *Biotechniques* **2007,** 43, (3), 354-9.
28. Schuck, P., Size-distribution analysis of macromolecules by sedimentation velocity ultracentrifugation and lamm equation modeling. *Biophys J* **2000,** 78, (3), 1606-19.
29. Trott, O.; Olson, A. J., AutoDock Vina: improving the speed and accuracy of docking with a new scoring function, efficient optimization, and multithreading. *J Comput Chem* **2010,** 31, (2), 455-61.